Characterization of aquatic groundwater colloids by a laser-induced breakdown detection and ICP-MS combined with an asymmetric flow field-flow fractionation

Min-Hoon Baik[†], Jong-Il Yun*, Muriel Bouby**, Pil-Soo Hahn and Jae-Il Kim**

Department of Radwaste Disposal Research, Korea Atomic Energy Research Institute, Daejeon 305-353, Korea
*Dept. of Nuclear & Quantum Engineering, Korea Advanced Institute of Science and Technology (KAIST), 371-1 Guseong-dong, Yuseong-gu, Daejeon 373-1, Korea
**Institut für Nukleare Entsorgung, Forschungszentrum Karlsruhe GmbH, P.O. Box 3640, D-76021 Karlsruhe, Germany
(*Received 22 June 2006 • accepted 12 February 2007*)

Abstract–This study investigated the characteristics of natural groundwater colloids by a laser-induced breakdown detection (LIBD) and inductively-coupled plasma mass spectrometry (ICP-MS) in a combination with an asymmetrical flow field-flow fractionation (AsymFFFF). The groundwater was sampled from a borehole in the Yuseong area of Daejeon, Korea at different geological depths from 30 to 460 m and its geochemical parameters were measured. The combination of AsymFFFF and LIBD revealed a heterogeneous size fraction with a relatively broad size distribution of the groundwater colloids. One of the size fractions of the groundwater colloids was about 20 nm up to smaller than 100 nm, and the other fractions were larger than 100 nm. The elemental composition of the groundwater colloids was also analyzed by the AsymFFFF coupled with an ICP-MS. Results from the ICP-MS coupled with the AsymFFFF provided us with information about the size-specific elemental composition. The smaller sized fractions mainly consisted of calcite colloids with strontium, whereas the larger fractions were comprised of colloids such as aluminosilicates and iron oxides. The observations of all the groundwater samples indicate a similar pattern for the colloid fractions in size and in element composition except in the concentration.

Key words: Groundwater Colloids, Laser-induced Breakdown Detection (LIBD), Asymmetric Flow Field-Flow Fractionation (AysmFFFF), Inductively-Coupled Plasma Mass Spectrometry (ICP-MS)

INTRODUCTION

Colloids have been known to transport contaminants over long distances and thus their potential roles in a contaminant migration in subsurface systems have been widely investigated [1-6]. Colloids in natural groundwaters are ubiquitous and composed of inorganic (e.g., silicates or clay minerals) or organic (e.g., humic substances and bacteria) materials and a composite of both as well. Their concentrations in natural groundwaters are generally in the 1-100 ppb range with an average diameter of the prevalent particles of less than 50 nm [2].

The heterogeneous nature of natural colloids, their low concentration, the extremely broad distributions of their size, and their tendency to form fragile aggregates makes it particularly difficult to measure their size distribution accurately [4]. In the past, most of the studies for the determination of colloid size distribution have been performed by a gravimetric determination of the fractions retained by filters of different nominal pore sizes [7]. However, this technique involves a very careful sample handling and processing, and thus it is likely to be affected by artifacts. Other techniques such as the Coulter counter [8], transmission electron microscopy (TEM) [9], and atomic force microscopy (AFM) [10] have also been used. In particular, photon correlation spectroscopy (PCS) has been widely applied to the determination of particle size distributions in natural waters. PCS is one of the most commonly applied nondestructive colloid sizing methods [11]. However, a conventional light scattering method may detect colloids of a relatively larger size in natural groundwaters (>50 nm), but it fails to detect colloids in laboratory water, since the method is not sensitive enough for a low concentration of very small particles.

Recently, a new sensitive method for direct detection of aquatic colloids has been developed that is capable of determining colloids which are small in size (<50 nm) and in a very low concentration (i.e., in the ppt range). The principle of the laser-induced breakdown detection (LIBD) system is based on the interaction of a focused pulsed laser beam with solid particles in the solution (see Fig. 1). At an appropriate power density (around 10^{10} W/cm^2), a dielectric breakdown which generates a plasma occurs selectively within the solid particles. The emitted light and shockwave accompanying the plasma formation can be detected for a determination of the colloid concentration and the average size [12,13]. Compared with the PCS, the detection sensitivity of this method for a particle diameter of about 20 nm is over a million-times superior [14]. The LIBD system is thus a very sensitive method for direct detection of the colloids in a solution.

The principles of LIBD are described in detail in the literature [12,13,15,16]. The power density required to induce the breakdown generating plasma is significantly lower for solid matter than for liquids. If the laser pulse power density (P_A) exceeds the breakdown threshold ($P_{A,cri}$) of colloids in a colloidal dispersion, the plasma will be generated almost exclusively on the colloids. The breakdown probability is defined as the number of measured breakdown events divided by the total number of laser pulses applied for each meas-

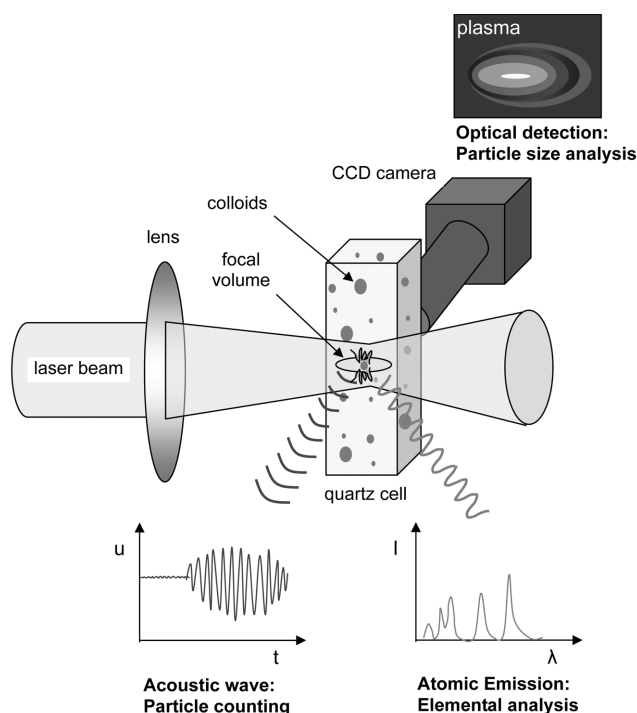[†]To whom correspondence should be addressed.
E-mail: mhbaik@kaeri.re.kr

Fig. 1. Principles of the laser-induced breakdown detection (LIBD).

urement and, therefore, can reach a value between 0 and 1 [13]. The breakdown probability is dependent on the P_A as well as particle concentration, size and material composition. The number of initial electrons produced by multiphoton absorption increases as the particles size increases [16]. Therefore, the breakdown probability at a given laser power density is proportional to the particle size. With increasing particle size, lower laser power density is needed to induce a dielectric breakdown on a particle.

For monodisperse particles, the laser pulse power density in a certain part of the focus volume is greater than or equal to the particle dependent breakdown threshold, $P_{A,crit}$. This region is defined as an effective focus volume, $V_{eff,F}$, of a particle. Thus the breakdown probability is also determined by the probability to find one or more particles within $V_{eff,F}$ during the laser pulse irradiation. The spatial distribution of the individual breakdown events within the focal area of the laser beam is found to be dependent on the particle diameter and independent of the particle concentration [12]. The width of the breakdown volume along the laser beam axis (effective focal length, L_z), therefore, can be taken as a measure for the mean colloid size. The effective focal length L_z is defined as the length in which 99.7% of the plasma events are found. To determine L_z, the light emission of single plasma is detected by a microscope charge-coupled device (CCD) camera system.

However, the characterization of colloids of a multimodal size distribution with an unknown composition is difficult to resolve from the LIBD alone. Particularly for the analysis of natural aquatic samples, a size fractionation prior to LIBD appears to be necessary to obtain quantitative results on the size and concentration of colloids [17]. Characterization of natural aquatic colloids by a flow field-flow fractionation (FFFF) has been described by a number of authors [17-22].

FFFF represents a colloid separation technique with no stationary phase required as, for example, in a size exclusion chromatography [23]. Thus, FFFF has lesser interaction effects of the sample components with an equipment surface. A separation of colloids is achieved in a laminar carrier flow under the action of a flow field, which is perpendicular to the carrier flow [23]. The movement of colloids in the laminar carrier flow is determined by their diffusion coefficient depending upon their size.

Also depending on the particle properties and the concentration, different detectors have been applied to record a particle size distribution, e.g., UV/VIS [20], laser light scattering (LLS) [19], LIBD [17-19], and inductively-coupled plasma mass spectrometry (ICP-MS) [14,18,21,24,25].

A combination of the FFFF with ICP-MS provides information on the inorganic element content of different colloid size fractions [21]. For an FFFF in this study, an asymmetric system (AsymFFFF) was chosen [22], because this device does not contain ceramic components that bleed aluminosilicate colloids in the carrier solution [20], as is the case for a conventional FFFF. The addition of LIBD as a detection system to the asymmetric flow field-flow fractionation (AsymFFFF) has been successfully applied to the character-
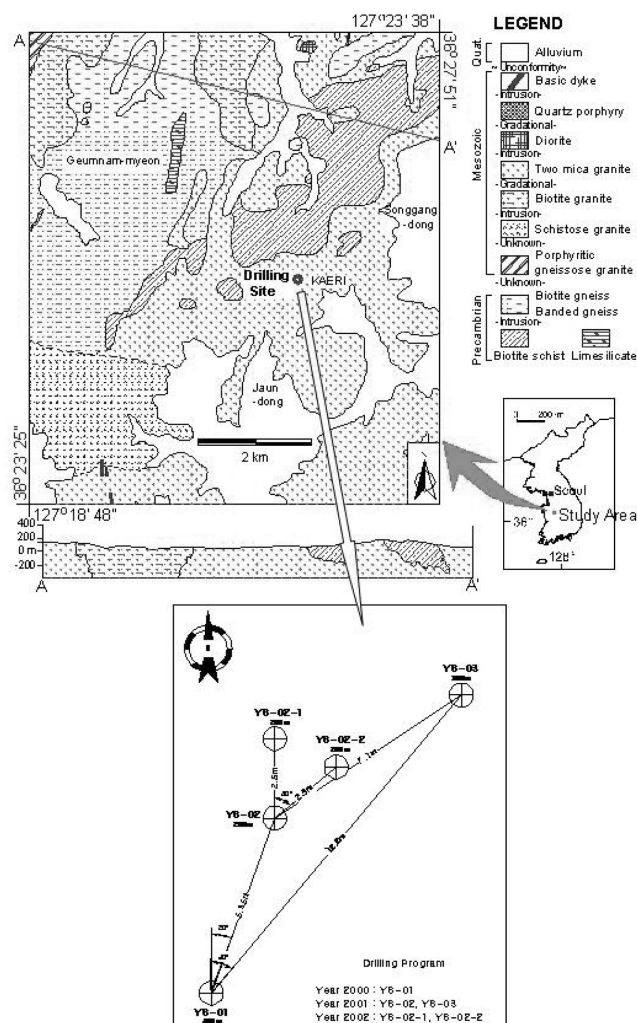
Fig. 2. Simplified geological map of Yuseong area, Daejeon, Korea and location of the borehole YS-01.

ization of humic colloids [18] and iron colloids [17].

Therefore, in this study, the groundwater colloids sampled from a borehole in the Yuseong area of Daejeon, Korea were characterized by LIBD and ICP-MS in a combination with AsymFFFF.

MATERIALS AND METHODS

1. Groundwater

The natural groundwater was sampled from a borehole located in Yuseong, Daejeon, Korea. Yuseong site is located at the Kum river drainage basin of the western peninsula, as shown in Fig. 2. The topography of the study site is characterized as rolling hills surrounded by upland of 300-500 m in height. The highest point in the area is about 850 m in height and most of the lowland is located at 50 m in height. The bedrock of the Yuseong area consists partly of the pre-Cambrian gneissic basement of 460 Ma old and Jurassic plutonic rocks of 160 Ma. The basement rock is composed mainly of biotite gneisses and schists in the northwestern region of the study area. The plutonic complex is composed of biotite granites, two mica granites and various dykes. Two-mica granite with a discernible foliation is a major rock type at the drilling site. The major minerals observed under a petrology microscope are quartz, plagioclase, biotite and mica with minor amounts of K-feldspar, chlorite and epidote [26].

Four boreholes of 76 mm in diameter were drilled at the Yuseong study sites (see Fig. 2). The length of the boreholes was about 200 to 500 m. A multi-packer (MP) system (Westbay Co, Canada) was installed in the selected borehole (YS-01) with 500 m in length from among the four boreholes for a groundwater monitoring. The borehole used for groundwater sampling was divided into 14 sections by packers according to the depth and fracture system. The groundwaters sampled from the YS-01 borehole at six different depths were

used for our study. The geochemical conditions of the six groundwater samples are listed in Table 1.

Groundwater was sampled by using a cylindrical stainless steel container with total volume of about 250 mL. This container has a valve for groundwater sampling which is electrically controlled by a controller on ground. The container is evacuated several times for sampling and then placed in a desired depth by a wire system through the borehole. When the container reaches a desired position isolated by a packer, the valve in the container is opened and then the groundwater around the container flows into the container by a pressure difference. After the container is raised by the wire system, the groundwater contained in the container is transferred to a sampling bottle which is carefully flushed several times by a highly pure nitrogen gas. Thus, the groundwater would not be contaminated by artifacts present in the borehole since the groundwater is not sampled by a pumping system but sampled by a multi-packer system at desired depths.

In the laboratory, filtration was performed by a membrane filter at a nominal pore size of 450 nm to separate precipitates from the groundwater samples. In particular, the brown color in the groundwater samples of YS-1-1 and YS-1-4 may have resulted from the higher amount of Fe concentration, not from humic substances, which can also be deduced from the ICP-MS results in Table 2. The samples show a relatively higher pH ranging from 8 to 12 which was measured in an inert gas atmosphere, with no significant pH change before and after the filtration. As shown in Table 2, the results from the ICP-MS measurements show that alkali and alkaline-earth metals are rich in the groundwaters. All of the experiments were carried out under aerobic conditions for simplicity.

The sample, YS-1-2, possesses a minimum amount of total carbon (TC) and inorganic carbon. Contrary to that, its filtrate reveals a relatively higher dissolved organic carbon (DOC). These TC-DOC

Table 1. Geochemical conditions of the groundwater sampled from the borehole YS-01

Sample	Depth (m)	Temp. (°C)	pH	Eh (mV)	EC (μS/cm)	DO (mg/L)	Alkalinity (×1,000)	log P_{CO_2} (atm)	TDS (mg/L)
YS-1-1	30.0	14.5	9.37	116	89	8.3	1.45	−4.59	161.3
YS-1-2	94.5	16.2	11.79	3	829	8.3	3.88	−9.97	135.7
YS-1-2	169.5	17.6	10.71	63	92	8.8	0.73	−7.19	87.7
YS-1-4	259.5	19.8	10.23	−109	91	7.6	0.96	−6.01	118.8
YS-1-5	367.5	22.4	9.95	−26	95	8.3	0.77	−5.63	110.2
YS-1-6	457.5	24.5	9.93	−142	92	9.6	0.75	−5.61	104.9

EC: electric conductivity, DO: dissolved oxygen, TDS: total dissolved solid

Table 2. Carbon concentrations and major ion concentrations of the groundwater samples analyzed by ICP-MS

Sample	TC (mg/L)	DOC (mg/L)	Concentrations of major ions (mg/L)				
			Na	Mg	K	Ca	Fe
YS-1-1	21.03	1.884	10.280	1.728	45.839	20.020	2.105
YS-1-2	4.996	2.115	30.408	0.006	s	45.710	Nd
YS-1-3	9.892	2.429	19.714	0.058	27.673	5.862	0.034
YS-1-4	11.11	1.682	s	0.795	29.836	19.164	3.788
YS-1-5	11.85	0.882	s	0.103	83.312	4.633	0.247
YS-1-6	12.68	1.2277	s	0.015	43.111	2.950	nd

s: saturated, nd: not detected

and ICP-MS result may correspond to those from LIBD as discussed later. The presence and stability of colloid-born species may be affected by a number of geochemical parameters, such as the pH, ionic strength, concentrations of the omnipresent cations like Na^+, Ca^{2+}, Mg^{2+}, $Fe^{2+/3+}$, and so on, and also the concentrations of the organic substances like humic and fulvic acids.
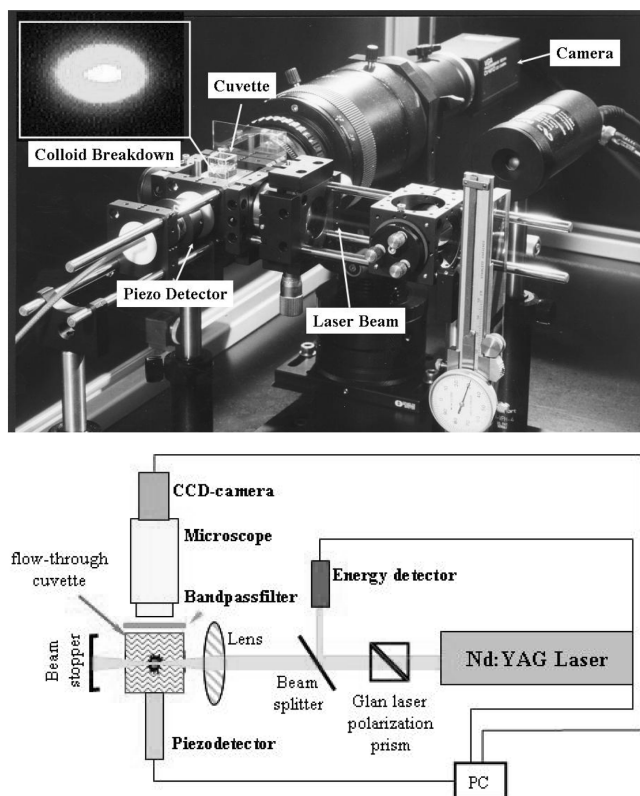
2. LIBD System

Fig. 3. Picture and schematic diagram of the LIBD system.

The measurement system for the LIBD is shown schematically in Fig. 3. The experimental system for the LIBD was originally constructed by INE/FZK (Institut für Nukleare Entsorgung, Forschungszentrum Karlsruhe) in Germany, and the system shown in Fig. 3 is one of the typical LIBD systems now available in INE/FZK. The experimental system used in this experiment is described in more detail elsewhere [12,17].

The LIBD system consists of a Q-switched, pulsed Nd-YAG laser (Continuum Surelite I) and a CCD camera coupled to a variable macro-microscope. A pulsed laser beam with a repetition rate of 20 Hz at the second harmonic wavelength of 532 nm is focused into a silica cuvette (Hellma, $10 \times 10 \times 30$ mm) containing the sample solution through a plano-convex lens of a 50 mm focal length. The pulse energy is adjusted to irradiance at 0.4 mJ by a variable attenuator. The plasma generated at a breakdown event is monitored by a macro-microscope equipped with a CCD monochrome camera triggered by the incident laser pulse and recorded by a PC controlled picture processing system.

The calibration of LIBD follows a two step procedure [13,14]. The LIBD was calibrated with several diluted commercial polystyrene reference particle dispersions (Polymer Standard Service GmbH, Polysciences Inc) with different particle sizes (19 nm-1,072 nm) prepared in a sample cell. Ultra-pure water from a MilliQ-UV-Plus apparatus (Millipore) with a resistivity of 18.2 MΩ-cm was used as a dispersion medium. Stock solutions of the reference particles were prepared by diluting the original reference colloid dispersions with ultra-pure water.

Applying the calibration procedure, an average particle diameter, d_p, for a given sample can be determined by measuring the effective focal length, L_z since L_z is linearly related with d_p. From d_p and the measured breakdown probability, the particle concentration can be calculated from the calibration curves obtained from the calibration procedure [12].

3. Colloid Size Fractionation

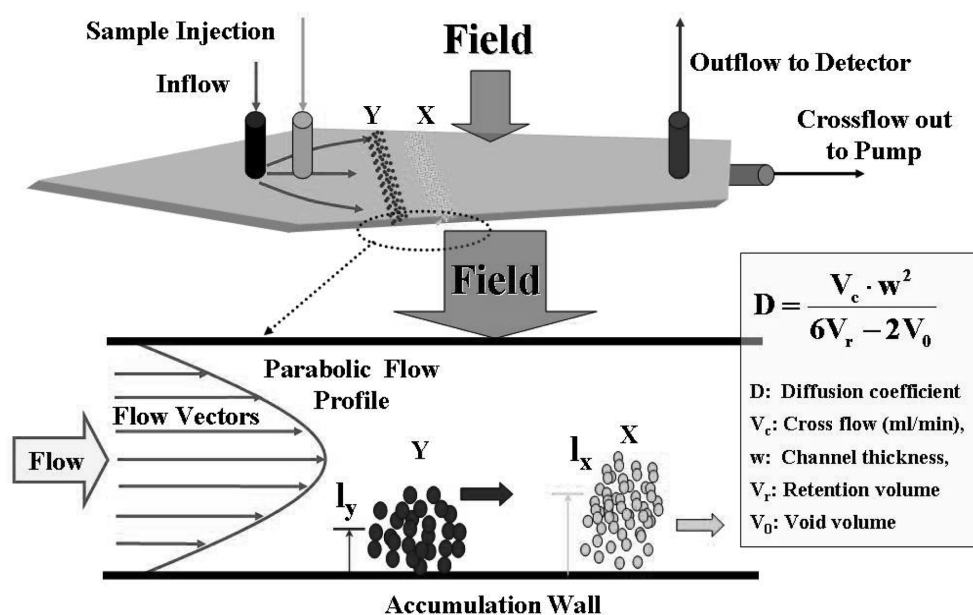Fig. 4 shows the principle and schematic diagram of the Asym-

Fig. 4. Detection principle and the schematic diagram of the AsymFFFF system.

FFFF system (HRFFF-10.000 AF4, Postnova Analytics). The accumulation wall consists of an ultrafiltration membrane (regenerated cellulose; Cutoff: 5 kDa; Schleicher & Schuell), and the upper wall is made of a plexiglass plate. A PTFE spacer restricts the area where the fractionation takes place. The fractionation channel volume, determined by injecting $NaNO_3$ (20 μL diluted to 0.01% in H_2O), is found to be 0.98±0.05 mL. The carrier solution was made of a 5 mmol/L Tris buffer solution at pH 8.6. The flow rates for the channel flow and cross flow were equally 0.5 mL/min for both. Injection volume of the sample was 500 μL. Polystyrene particles of 5 ppb (20 nm) and 10 ppm (100 nm) were used as reference colloids.

4. Combined Detection System

For the analysis of inorganic components of groundwater colloids, the effluent from the AsymFFFF is mixed through a T-piece with 5% nitric acid containing 50 μg/L Rh as an internal standard and introduced into ICP-MS (Perkin-Elmer, Elan 6000) at a constant rate of 0.5 mL/min similar to the method described in the literature [25]. The average size of the fractionated colloids is determined by passing a portion of the effluent (750 μL) through a flow-through cell of the LIBD system. Each breakdown probability is evaluated by averaging the breakdown events observed with 80 laser pulses. The resulting fractogram is plotted as a function of the elution volume.

RESULTS AND DISCUSSION

1. Characterization with LIBD

The groundwater samples filtered by a microfilter of 450 nm were measured by using an LIBD system. Measurement results of the LIBD system for the groundwater samples, reference latex particles, and Milli-Q water are shown in Fig. 5. In Fig. 5, the slope of a breakdown curve in a linear region corresponds to the particle number density, i.e., the concentration of colloidal particles and the breakdown threshold energy in the x-axis depends on the average diameter of the colloids as mentioned previously. With the exception of one sample, YS-1-2, the results from the LIBD measurement
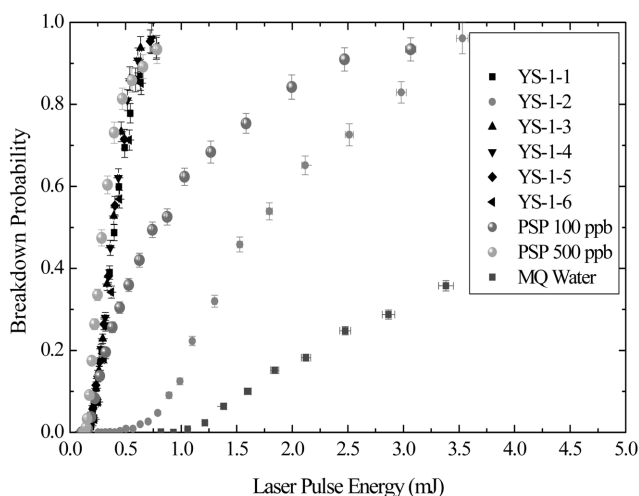
for all the groundwater samples are similar for the breakdown behaviour. According to the existing calibration curves, which have been carried out with latex particles as a reference colloid, the particle size of the groundwater samples was estimated to be around 400 nm. Then so-called S-curves of the 404 nm latex particles with two different particle concentrations (i.e., 100 and 500 ppb) were measured. The result is consistent with that from the predicted particle size of the groundwater samples. According to the same calibration curve, the sample YS-1-2 shows an average particle size of about 220 nm.

Additionally, the LIBD result of the sample, YS-1-6, reveals a slightly smaller average particle size than the rest of the samples, YS-1-1, YS-1-3, YS-1-4 and YS-1-5, that were identified to have the same particle size and particle number density within the measurement uncertainty. The results presumably show a cut-off effect of a filtration with a pore size of 450 nm. The largest fraction of the colloids may considerably influence the breakdown threshold and the probability and cause a misleading data interpretation.

It can be assumed that each sample has a multi-modal distribution of the particles. This multi-modal distribution of the groundwater colloids can be handled and analyzed by AsymFFFF coupled with LIBD. Nevertheless, we have evaluated the particle concentration to be about 290 ppb. The material dependency of the LIBD measurement was not considered for the evaluation of the particle size and the concentration of the groundwater colloids. As it has been widely known, the material dependency of the LIBD measurement is one of the greatest challenges regarding the quantification of unknown and/or mixed colloidal particles.

2. Characterization with AsymFFFF Combined with LIBD

Fig. 5. Measurement results of the LIBD for the groundwater samples, reference latex particles (PSP, 404 nm in diameter), and Milli-Q water (MQ).
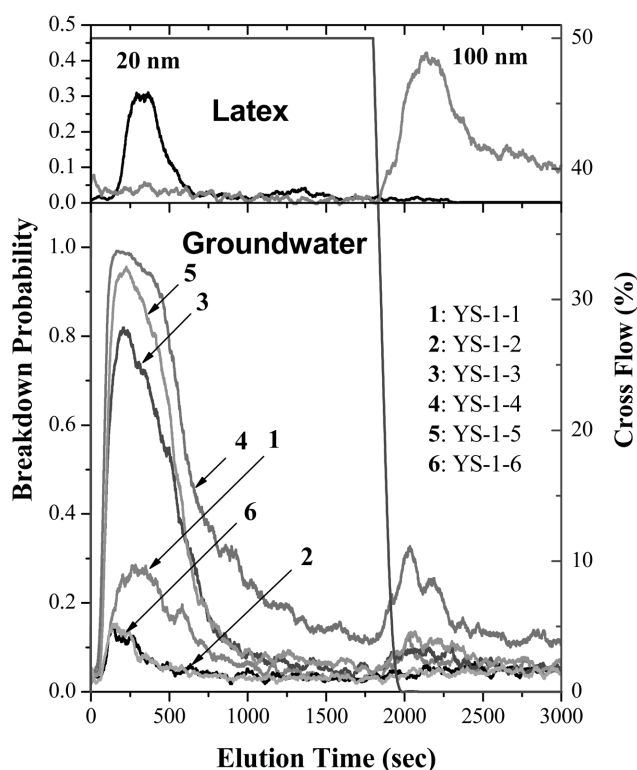

Fig. 6. Colloid characterization results for the groundwater samples by the AsymFFFF coupled with a LIBD.

Fig. 6 shows the results of the AsymFFFF fractionation as a function of the particle size, which was analyzed by LIBD. The effluent is placed into the LIBD system to evaluate the colloid number density by measuring the breakdown probability. The results show that there are two main fractions: the first one is between 20 and <100 nm, and the second one ranges from 100 to 450 nm. The LIBD results of the fractionated colloid sizes in Fig. 6 are found to be somewhat larger than the estimated average size evaluated only by the LIBD system shown in Fig. 5. Relatively lower colloid concentrations in samples YS-1-2 and YS-1-6, compared to samples YS-1-3, YS-1-4 and YS-1-5, were observed.

Thus the application of LIBD system in combination with Asym-FFFF may be helpful to determine the size distribution of aquatic colloids. Unfortunately, the equipment was calibrated up to a particle size smaller than 200 nm. The determination of larger particles is possible after a new parameter optimization (cross flow etc.) and calibration with reference particles in a corresponding particle size range.

3. Characterization with AsymFFFF Combined with ICP-MS

The polyvalent element distribution in natural groundwater colloids of different sizes as fractionated by Asym-FFFF and then detected by ICP-MS was analyzed for the groundwater sample YS-1-4, for instance. Fig. 7 shows the results of the asymFFFF fractionation as a function of the particle size, which was analyzed by ICP-MS for the elution profiles of Ca^{133}, Fe^{57}, Si^{28}, Sr^{88}, and Ca^{44} originally present in the groundwater colloids. The detected ions per second (intensity=counts per second, CPS) are given as relative element signals. The particles of a smaller size are eluted at the beginning in Asym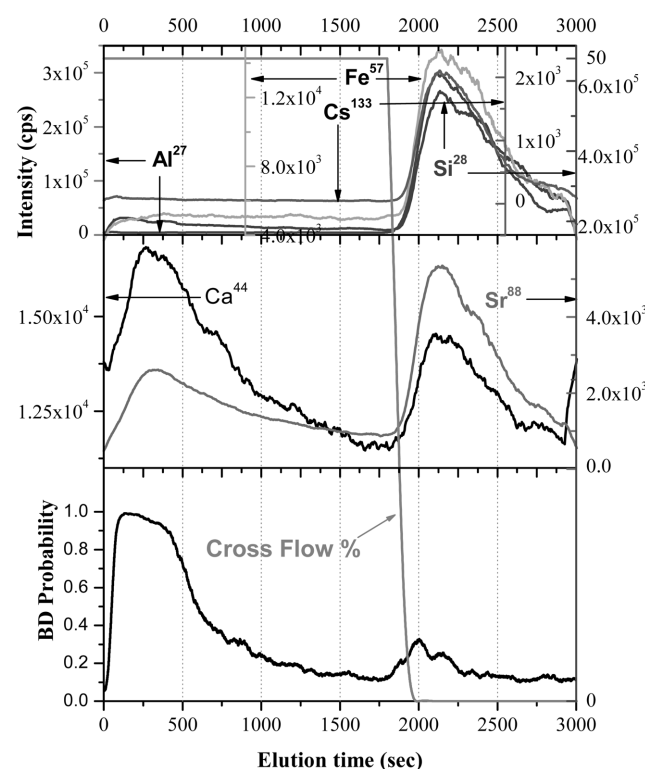FFFF whereas the larger particles appear at a later stage. It was found that the calcite colloids were present with strontium (saturated), and aluminosilicate colloids and that the Fe-colloids were mainly present in the larger colloid fractions. However, the origin of the groundwater colloids is not clear due to a lack of data.

CONCLUSIONS

In this study, the groundwater colloids sampled from a borehole in the Yuseong area of Daejeon, Korea were characterized by the LIBD and ICP-MS in a combination with AsymFFFF. The LIBD system could determine not only the average size but also the average concentration of the groundwater colloids. It was estimated from the LIBD measurements that the average size and concentration of the groundwater colloids were about 400 nm and 290 ppb, respectively.

The combined measurement of AsymFFFF and LIBD for the groundwater colloids showed heterogeneous size fractions with a relatively broad size distribution. The smaller size fractions were comprised of about 20 nm up to smaller than 100 nm, and the other fractions were larger than 100 nm. As a result, the combination of LIBD and AsymFFFF appears to be a helpful tool for the characterization of colloid dispersions with particle concentrations in the upper ppt range. The combination of AsymFFFF and ICP-MS provided information about the elemental composition of the fractionated colloids. A smaller fraction of the groundwater colloids with calcite was present with Sr (saturated) and a larger fraction was mainly present as aluminosilicate colloids and Fe-colloids. However, the origin of the groundwater colloids is not clear due to a lack of data.

In conclusion, the combined measurement systems of LIBD and ICP-MS with AsymFFFF appear to be a very useful method for characterization of groundwater colloids, especially for the size distribution and composition of the groundwater colloids.

Fig. 7. Colloid characterization results for the selected groundwater sample YS-1-4 by AsymFFFF coupled with ICP-MS.

REFERENCES

1. O. Atteia, D. Perret, T. Adatte, R. Kozel and P. Rossi, *Environ. Geol.*, **34**, 257 (1998).
2. C. Degueldre, I. Triay, J. I. Kim, P. Vilks, M. Laaksharju and N. Miekeley, *Appl. Geochem.*, **15**, 1043 (2000).
3. A. B. Kersting, D. W. Efurd, D. L. Finnegan, D. J. Rokop, D. K. Smith and J. L. Thompson, *Nature*, **397**, 56 (1999).
4. J. I. Kim, *Radiochim. Acta*, **52/53**, 71 (1991).
5. J. F. McCarthy and J. M. Zachara, *Environ. Sci. Technol.*, **23**, 496 (1989).
6. P. Vilks, H. Miller and D. Doern, *Appl. Geochem.*, **6**, 553 (1991).
7. J. Buffle and G. G. Leppard, *Environ. Sci. Technol.*, **29**, 2169 (1995).
8. C. Degueldre, B. Baeyens, W. Goerlich, J. Riga, J. Verbist and P. Stadelman, *Geochim. Cosmochim. Acta*, **53**, 603 (1989).

9. A. Lerman, K. L. Carder and P. R. Betzer, *Earth Planetary Sci. Lett.*, **37**, 61 (1977).

10. M. Plaschke, J. Römer, R. Klenze and J. I. Kim, *Coll. Surf. A*, **160**, 269 (1999).

11. M. Filella, J. Zhang, M. E. Newman and J. Buffle, *Coll. Surf. A*, **120**, 27 (1997).

12. T. Bundschuh, R. Knopp and J. I. Kim, *Coll. Surf. A*, **177**, 47 (2001).

13. T. Bundschuh, W. Hauser, J. I. Kim, R. Knopp and F. Scherbaum, *Coll. Surf. A*, **180**, 285 (2001).

14. M. Plaschke, T. Schäfer, T. Bundschuh, T. N. Mahn, R. Knopp, H. Geckeis and J. I. Kim, *Anal. Chem.*, **73**, 4338 (2001).

15. T. Kitamori, K. Yokose, K. Suzuki, T. Sawada and Y. Gohshi, *Jpn. J. Appl. Phys.*, **27**, 983 (1988).

16. F. J. Scherbaum, R. Knopp and J. I. Kim, *Appl. Phys. B*, **63**, 299 (1996).

17. M. Bouby, H. Geckeis, T. N. Manh, J. I. Yun, K. Dardenne, T. Schäfer, C. Walther and J. I. Kim, *J. Chromatography A*, **1040**, 97

18. M. Bouby, T. N. Manh, H. Geckeis, F. Scherbaum and J. I. Kim, *Radiochim. Acta*, **90**, 727 (2002).

19. T. N. Manh, R. Knopp, H. Geckeis, J. I. Kim and H. P. Beck, *Anal. Chem.*, **72**, 1 (2000).

20. T. N. Manh, H. Geckeis, J. I. Kim and H. P. Beck, *Coll. Surf. A*, **181**, 289 (2001).

21. H. Prestel, L. Schott, R. Niessner and U. Panne, *Water Res.*, **39**, 3541 (2005).

22. M. E. Schimpf and M. P. Pettys, *Coll. Surf. A*, **120**, 87 (1997).

23. J. C. Giddings, *Science*, **260**, 1456 (1993).

24. H. Geckeis, T. N. Manh, M. Bouby and J. I. Kim, *Coll. Surf. A*, **217**, 101 (2003).

25. M. Hasselöv, B. Lyven, C. Haraldsson and W. Sirinawin, *Anal. Chem.*, **71**, 3497 (1999).

26. G. Y. Kim, Y. K. Koh, D. S. Bae and C. S. Kim, *J. Miner. Soc. Korea*, **17**, 99 (2004).